RSC Advances

This article can be cited before page numbers have been issued, to do this please use: S. Kakogianni, M. A. Lebedeva, G. Paloumbis, A. K. Andreopoulou, K. Porfyrakis and J. Kallitsis, *RSC Adv.*, 2016, DOI: 10.1039/C6RA22857G.

ROYAL SOCIETY OF CHEMISTRY

www.rsc.org/advances

View Article Online
DOI: 10.1039/C6RA22857G

Journal Name

ARTICLE

Semiconducting End-Perfluorinated P3HT-Fullerenic Hybrids as Potential Additives for P3HT/$IC_{70}BA$ blends

Received 00th January 20xx,
Accepted 00th January 20xx

DOI: 10.1039/x0xx00000x

www.rsc.org/

S. Kakogianni,[a] M. A. Lebedeva,[b] G. Paloumbis,[c] A. K. Andreopoulou,[a,d] K. Porfyrakis,[b] and J. K. Kallitsis[a,d,*]

An efficient route to synthesise hybrid polymers consisting of a semiconducting polymer and a fullerene unit, for BHJ OPV devices is presented herein. The synthetic procedure is based on the in situ functionalisation of regioregular polythiophenes of various molecular weights with perfluorophenyl moieties at the ω end position of the polymeric chains, after the GRIM polymerisation reaction. Each of the perfluorophenyl moieties is then decorated with an azide group, and employed in a [3+2] cycloaddition reaction with fullerene species, i.e. C_{70} or $IC_{70}MA$, yielding P3HT-fullerene hybrids covalently linked via aziridine bridges. The effectiveness of the purification procedures of the above organic and hybrid materials were evaluated by extended spectroscopic and chromatographic methods. The optical and electrochemical characterisation of the resulting hybrid structures revealed that the unique optoelectronic properties of the P3HT polymers are retained in the hybrid materials. Whereas the morphological properties are largely affected by the introduction of the C_{70} and $IC_{70}MA$ fullerenes. The enhanced and tunable nanophase separation observed in the polymer-fullerene hybrid films coupled with their excellent optoelectronic properties makes them exciting potential polymeric additives for the P3HT:$IC_{70}BA$ active blends.

Introduction

Low-cost organic photovoltaics hold significant potential for meeting future electricity demands and have steadily approached economic feasibility in recent years.[1,2,3] One of the most efficient device architecture is bulk heterojunction (BHJ) solar cells in which the donor and the acceptor components are blended together to form a bicontinuous interpenetrating network.[4,5] In order to achieve highest power conversion efficiencies (PCEs), the choice of the donor and the acceptor materials in such devices is crucial and both the electronic structure and the morphology[6] of the resulting mixture have to be considered. Among the most widely used electron donating polymers,[7,8] the regioregular poly(3-hexylthiophene) (*rr*-P3HT) is by far the most commonly studied due to both relatively easy and cost efficient preparation and electronic properties matching the demand of the device architecture.[9] The state of the art electron acceptor components are various C60 fullerene derivatives.[10] The typical BHJ devices comprise a mixture of P3HT and [6,6]-phenyl-C_{61}-butyric acid methyl ester ($PC_{61}BM$) and exhibit moderate power conversion efficiencies (PCEs) of 4-5 % which is significantly lower than desired. Thermal treatment[11,12] or solvent and vapour[13] annealing, as well as mixture solvent treatment[14,15] led to improved nano-scaled morphology of the active layer and so to slightly higher efficiencies. New generation fullerene acceptors, based on the bis-functionalisation pattern of the fullerene cage[16,17,18] as well as the replacement of C_{60} fullerene with the stronger absorbing C_{70},[16] and the incorporation of slightly electron donating indene groups,[19] resulted in the highly efficient acceptors indene-C_{70} mono- and, most importantly, bis-adducts ($IC_{70}MA$ and $IC_{70}BA$ respectively).[20] As a result, the LUMO level in $IC_{70}BA$ is 0.19 eV higher as compared to PCBM and 0.07 eV compared to the analogous bis-PCBM adducts.[16] Consequently, the BHJ devices featuring the P3HT:$IC_{70}BA$ mixtures show remarkably high Voc of 0.86 V and average PCEs of 6.5 %,[20] and upon further optimization of the morphology of the active layer[21,22] and device architecture[23,24] have achieved PCEs as high as 7.40%. The performance of such devices can be further improved by the stabilization and control over the morphology of the P3HT:fullerene active blends. This can be achieved through several approaches: (1) functionalisation of either the electron donor or electron acceptor with different functional groups to affect the miscibility and thus co-crystallization in the blend;[25,26,27,28] (2) employing various thermal or solvent annealing steps which both improve the nanophase separation,[11,29,30] or (3) incorporation of hybrid materials, consisting of a

[a] Department of Chemistry, University of Patras, 26504 Patras ,Greece
[b] Department of Materials, University of Oxford, 16 Parks Road, Oxford, UK, OX1 3PH.
[c] Advent Technologies SA, Patras Science Park, Stadiou str., Platani, GR-26504, Greece.
[d] Foundation for Research and Technology Hellas/ Institute of Chemical Engineering Sciences (FORTH/ICE-HT), Platani Str., Patras, GR26504, Greece.
† Electronic Supplementary Information (ESI) available: Synthetic procedures, characterization via HPLC, ATR, TGA, UV-Vis, PL, TEM, CV. See DOI: 10.1039/x0xx00000x

View Article Online
DOI: 10.1039/C6RA22857G

semiconducting polymer and a carbon nanostructure, as compatibilisers of the polymer/fullerene binary blend[25,31,32,33,34,35] or (4) non-covalent interactions between compatibilisers bearing nitrogen heterocycles (such as pyridine-units) and the fullerene acceptor of the active blend.[36,37,38] Incorporation of small amounts (1-20 wt %) of such compatibilisers in the polymer:fullerene blend affects the morphology of the final blend and enhances phase stability between the major components. Various synthetic strategies have been exploited for the preparation of such hybrid polymeric architectures, mostly employing multi-step synthetic procedures as well as the introduction of non-conjugated connecting bridges between the semiconducting polymer and the carbon nanostructure. Recently developed new synthetic approaches instead utilise the "direct" attachment of the semiconductor to the fullerene cage via diamino-,[39] cyclopentadienyl-,[40] or aziridine-[41,42,43] functional groups resulting in nearly fully conjugated systems.

In this work, we focus on the development of such hybrid polymeric materials based on a previously reported methodology.[41] More specifically, the electron deficient perfluorophenyl moiety is introduced at the ω end position of regioregular-P3HT oligomers, during the polymerization step, in high yields followed by the substitution of one of the fluorine groups with the highly reactive azide functionality. Afterwards, the azide moiety perfoms a [3+2] cycloaddition reaction with a fullerene specie, either C_{70} or $IC_{70}MA$, affording the hybrid semiconducting poly(thiophene). Extensive purification and combined structural characterization was performed for the polymeric precursors and the final hybrid materials to ensure the successful introduction of the fullerenes onto the P3HT polymeric chains. The optical, electronic and morphological properties of the final hybrid materials revealed potential application of these polymers as additives of the P3HT:$IC_{70}BA$ based BHJ OPVs devices.

Experimental Section

2.1. Materials

Fullerene Carbon (C_{70}, 99.5%) was purchased from SES research. Tetrahydrofuran (THF) was purchased from Aldrich and dried by distillation with benzophenone and metallic sodium (THFdry). All the other solvents and reagents were purchased from Aldrich and used without further purification unless otherwise stated.

2.2. Instrumentation

^{1}H, ^{13}C, ^{19}F, ^{15}N NMR spectra were recorded on a Bruker Advance DPX 400.13, 100.6 and 376.5, 40.55 MHz spectrometer, respectively, using $CDCl_3$ as solvent containing TMS as internal standard.

Size Exclusion Chromatography (SEC) measurements were carried out using a Polymer Lab chromatographer equipped with two PLgel 5 µm mixed columns and a UV detector, using $CHCl_3$ as an eluent with a flow rate of 1 mL/min at 25 ^{o}C, molecular weight calibration versus polystyrene standards. The UV-Vis detector was set at 440 nm were the maximum absorbance wavelength of *rr*-P3HT is located.

ATR spectra were recorded on a "Bruker Optics' Alpha-P Diamond ATR Spectrometer of Bruker Optics GmbH".

High performance liquid chromatography (HPLC) was performed on a Japan Analytical Industry (JAI) LC-9103 Recycling Preparative HPLC with a modular Hitachi L-7150 pump and JAI UV Detector 3702 (Cosmosil® Buckyprep-M 20.0 mm ID x 250 mm column, toluene, 16 ml min-1 flow rate, 312 nm absorption detector).

Matrix-assisted laser desorption/ionization time-of-flight mass spectra (MALDI-TOF MS) of the fullerene-containing samples were obtained on a Bruker microflex™ LT spectrometer (negative ionization, trans-2-[3-(4-t-butyl-phenyl)-2-methyl-2-propenylidene]malononitrile (DCTB) matrix).

UV-Vis spectra were recorded using a Hitachi U-1800 spectrophotometer. Continuous wave photoluminescence was measured on a Perkin Elmer LS45B spectrofluorometer.

Cyclic voltammetric studies were carried out using an Autolab PGSTAT302N potentiostat, in a three-electrode arrangement in a single compartment cell. A glassy carbon working electrode, a Pt wire secondary electrode and a saturated Ag/AgCl reference electrode (chemically isolated from the test solution via a bridge tube containing electrolyte solution and fitted with a porous Vycor frit) were used in the cell. Experiments were performed under an atmosphere of argon and in anhydrous solvents. Sample solutions were prepared under an atmosphere of argon using Schlenk line techniques and consisted of a 0.2 M [$^{n}Bu_4N$][BF_4] solution as the supporting electrolyte and a 0.5-1 mM solution of the test compound. Redox potentials were referenced vs. the Fc^{+}/Fc couple, which was used as an internal standard. Compensation for internal resistance was not applied.

Transmission electron microscopy (TEM) measurements were performed on a JEOL JEM2100 operating at 200 kV. Sample preparation for TEM examination involved the preparation of dilute solutions of the samples in o-DCB and filtration through a 0,45 µm filter. A drop of the solution was placed on 3 mm carbon coated copper grids (Electron Microscopy Sciences) and the samples were dried in air for 2 days. Image post-analysis of the hybrid polymers was performed in ImageJ.[44,45]

2.3. Synthetic procedures

end *rr*-P3HT-5F (*high MW*, n=80): 2,5-Dibromo-3-hexyl-thiophene (24.22 g, 74.26 mmol) was dissolved in THFdry (320 mL) in a round-bottom two-neck flask equipped with a stirring bar and a reflux condenser under argon atmosphere. MeMgCl (3 M solution in THF, 25 mL, 75 mmol) was added, and the reaction mixture was heated to reflux for 2 h. After cooling to room temperature, Ni(dppp)Cl_2 (322 mg, 0.594 mmol) was added, and the reaction mixture was heated to reflux for 4 h. Pentafluorophenyl magnesium bromide (0.5 M solution in diethyl ether, 20 mL, 14.85 mmol) was then added to the hot reaction mixture, and the mixture was refluxed for additional 16 h. The polymer was cooled to room temperature and then precipitated in MeOH (2.5 Lt), filtered, and the resulting

View Article Online
DOI: 10.1039/C6RA22857G

precipitate was purified by Soxhlet extraction using MeOH, followed by acetone, *n*-hexane and $CHCl_3$. The chroroform fraction was concentrated to 30 mL and precipitated in MeOH (2 Lt). The resulting precipitate was filtered and dried in air to give the product in 48% yield (6 g). Regioregularity 98% (calculated from ^{1}H NMR spectrum) ^{1}H NMR (δH; $CDCl_3$; Me_4Si): 6.98 (s, 1H), 2.80 (t, 2H), 1.70 (m, 2H), 1.44-1.35 (two broad, 6H), 0.92(t, 3H). ^{13}C NMR (δC; $CDCl_3$; Me4Si): 139.9, 133.7, 130.5, 128.6, 31.7, 30.5, 29.5, 29.3, 22.7, 14.1. ^{19}F NMR (δF; $CDCl_3$; Me_4Si): -110.52, -129.28, -136.41.

end *rr*-P3HT-5F-N_3 (*high MW*, n=80): end *rr*-P3HT-5F (500 mg, 0.25 mmol) was dissolved in dry THF (10 mL), and thoroughly degassed with argon. A solution of NaN_3 (60 mg, 0.59 mmol) and 18-crown-6 (240 mg, 0.91 mmol) in dry DMF (6 mL) was then added, and the resulting mixture degassed and filled with Ar and heated to 40 ^{o}C for 48 h. The mixture was then precipitated into a mixture of deionized water:methanol 1:1 (200 mL). The resulting precipitate was then separated by filtration, washed with deionized water (5 x 20 mL) and dried under vacuum at 30 ^{o}C overnight to give the product (490 mg, 98%). ^{1}H NMR (δH; $CDCl_3$; Me_4Si): 6.99 (s, 1H), 2.81(t, 2H), 1.70 (m, 2H), 1.44-1.35 (two broad, 6H), 0.92 (t, 3H). ^{13}C NMR (δC; $CDCl_3$; Me_4Si): 139.9, 133.7, 130.5, 128.6, 31.7, 30.5, 29.5, 29.3, 22.7, 14.1. ^{19}F NMR (δF; $CDCl_3$; Me_4Si): -135.8, -136.4. ^{15}N NMR (δN; $CDCl_3$; Me_4Si): 232.9, 52.20.

end *rr*-P3HT-5F-N-C_{70} (*low MW*, n=6): end *rr*-P3HT-5F-N_3 (150 mg, 0.97 mmol) and C_{70} (116 mg, 0.97 mmol) were dissolved in *o*-DCB (50 mL), and thoroughly degassed and filled argon. The reaction mixture was then heated to 140 ^{o}C for 72 h. The solvent was then removed, and the resulting solid was treated THF at room temperature for 24 h in order to remove traces of unreacted C_{70}. The mixture was then filtered through celite, and the filtrate was concentrated to dryness under reduced pressure. The resultant solid was dried under vacuum at 50 ^{o}C overnight to yield the product (155 mg, 60%). ^{1}H NMR (δH; $CDCl_3$; Me_4Si): 6.99 (s, 1H), 2.81 (t, 2H), 1.71 (m, 2H), 1.44-1.35 (two broad, 6H), 0.91 (t, 3H). ^{13}C NMR (δC; $CDCl_3$; Me_4Si): 150.5, 147.9, 147.2, 145.2, 144.2, 143.7, 143.5, 143.3, 143.1, 142.9, 140.4, 140.2, 139.9, 139.8, 139.6, 138.1, 135.8, 135.8, 133.9, 133.7, 133.5, 131.5, 131.0, 130.7, 130.6, 130.5, 128.8, 128.6, 128,5, 128.3, 128.2, 128.1, 127.2, 127.1, 126.6, 125.5, 31.7, 30.5, 29.5, 29.3, 22.7, 14.1. ^{19}F NMR (δF; $CDCl_3$; Me_4Si): -136.2, -135.6. ^{15}N NMR (δN; CDCl3; Me_4Si): 148.2.

end *rr*-P3HT-5F-N-IC_{70}MA (*medium MW*, n=12): end *rr*-P3HT-5F-N_3 (200 mg, 0.099 mmol) and IC_{70}MA (95 mg, 0.099 mmol) were dissolved in *o*-DCB (65 mL), and thoroughly degassed and filled argon. The reaction mixture was then heated to 140 ^{o}C for 72 h. The solvent was concentrated to 20 mL, and the mixture was then precipitated in Et_2O and stirred at room temperature for 72 h in order to remove traces of unreacted IC_{70}MA. The mixture was then filtered through Nylon filter, and the resultant solid was dried under vacuum at 50 ^{o}C overnight to yield the hybrid material (150 mg, 50%). ^{1}H NMR (δH; $CDCl_3$; Me_4Si): 6.99 (s, 1H), 2.81 (t, 2H), 1.71 (m, 2H), 1.44-1.35 (two broad, 6H), 0.91 (t, 3H). ^{19}F NMR (δF; $CDCl_3$; Me_4Si): -136.2 -130.4, -136.44. ^{15}N NMR (δN; $CDCl_3$; Me_4Si): 200.

Results and discussion

We have recently reported a versatile approach for creating semiconducting polymer-fullerene hybrid structures based on the [3+2] cyloaddition reaction of perfluorophenylazide tagged semiconducting small molecules or polymers and C_{60}-fullerene derivatives. This method is straightforward and high yielding, and has been successfully employed for the functionalization of pristine C_{60} as well as of the C_{60} derivative, $PC_{61}BM$ in good yields.[41] We have therefore utilized the same methodology in the present study for the preparation of C_{70}-containing hybrid polymers. To assess the reactivity of C_{70} and develop the procedure for C_{70} functionalisation with semiconducting polymers, we have initially performed a model reaction between C_{70} and a small molecule, namely phenyl perfluorophenylquinoline azide (Ph-5FQ-N_3) (Scheme S1). The [3+2] cycloaddition reaction between the Ph-5FQ-N_3 and the C_{70} was performed in o-dichlorobenzene (*o*-DCB) at 140 ^{o}C, followed by chromatographic purification (eluents: petroleum ether, petroleum ether:toluene gradient mixtures) to give the Ph-5FQ-N-C_{70} hybrid in good yields (60 %). The structure of the Ph-5FQ-N-C_{70} hybrid was confirmed by a combination of ^{13}C NMR, ATR, UV-Vis and PL spectroscopies proving the successful functionalisation of C_{70} via the perfluorophenyl aziridine bridge formation (see SI file for details).

This methodology was then transferred to the *rr*-P3HT precursors for the preparation of P3HT-fullerene hybrids. We initially synthesized ω end perfluorophenyl regioregular poly(3-hexylthiophenes) (*rr*-P3HT-5F) of different molecular weights, which were then transformed to azides followed by the [3+2] cycloaddition reaction with the C_{70} or IC_{70}MA fullerenes to yield the corresponding P3HT–fullerene hybrid semiconducting polymers.

3.1. Synthesis and Characterization of P3HT-hybrids

a) Preparation of azide P3HT-5F precursors

End functionalized perfluorophenyl regioregular-polythiophene (*rr*-P3HT-5F) can be synthesized in two ways. The first method involves a Suzuki cross coupling reaction of a perfluorophenylboronic acid with the "living" bromide end groups of *rr*-P3HT chains[46] produced via the GRIM polymerization. The second method, which was used in this study involves, the in situ addition of perfluorophenylmagnesium bromide directly in the polymerization medium after the completion of the GRIM polymerization step (Scheme 1).[28] The successful introduction of the perfluorophenyl ring was confirmed through ^{19}F NMR and ATR spectroscopies (Figures S8, 1). The ^{19}F NMR spectrum of *rr*-P3HT-5F presents three peaks at -100.51, -130.46, -136.41 ppm corresponding to the pentafluorophenyl unit (Figure S8). Additionally, the ATR spectrum of the end *rr*-P3HT-5F presents a strong band at 1250 cm^{-1} and two strong bands at 1020-1090 cm^{-1}, which are absent in the non-functionalized P3HT. These bands are attributed to the vibration of C-F bond and the vibration of the phenyl ring respectively (Figure 1), confirming the successful introduction of the perfluorophenyl unit at the end of the P3HT chain.

View Article Online
DOI: 10.1039/C6RA22857G

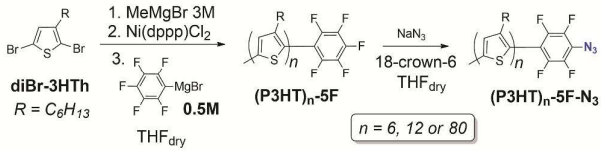

Scheme 1. Synthetic route towards the *end* perfluorophenyl functionalized P3HT ((P3HT)$_n$-5F) and the corresponding azide tagged polymer ((P3HT)$_n$-5F-N$_3$).

In order to investigate the influence of the molecular weight (MW) of the P3HT on the properties of the targeted hybrid materials, end *rr*-P3HT-5F with different molecular weight (*low MW* n=6*, medium MW* n=12*, high MW* n=80) have been synthesized. The preparation of the *low* and *medium MW* end P3HTs was achieved by performing the polymerization reaction using an increased amount of the Ni-catalyst (Ni(dppp)Cl$_2$) to the monomer (M), corresponding to a ratio of [M]:[catalyst]=50:1 in contrast to the typical ratio of 136:1. The crude end P3HT-5F was then purified via Soxhlet extraction using methanol, followed by acetone, hexane and chloroform as solvents.

The *low MW* end P3HT-5F (n=6) was obtained from the hexane extract while the *medium MW* end P3HT-5F (n=12) proceeded from the CHCl$_3$ fraction. The *high MW* end P3HT-5F (n=80) polymer was synthesized in the same manner using the [M]:[catalyst]=125:1 ratio and was isolated from the CHCl$_3$ fraction of the Soxhlet purification procedure. The resulting end P3HT-5F polymers were characterized, in respect to their molecular characteristics, by SEC revealing that the polymers synthesized herein are of narrow polydispersities of ~1.3. Moreover, by ^{1}H NMR spectroscopy the relative integral intensities of the thiophene protons at 6.99 ppm and of the α-methylene protons at 2.58 ppm were used to calculate the average thiophene repeating units in each case namely of 6, 12 and 80 thiophene repeating units for the *low MW*, *medium MW* and *high MW* polymers, respectively (Table 1).

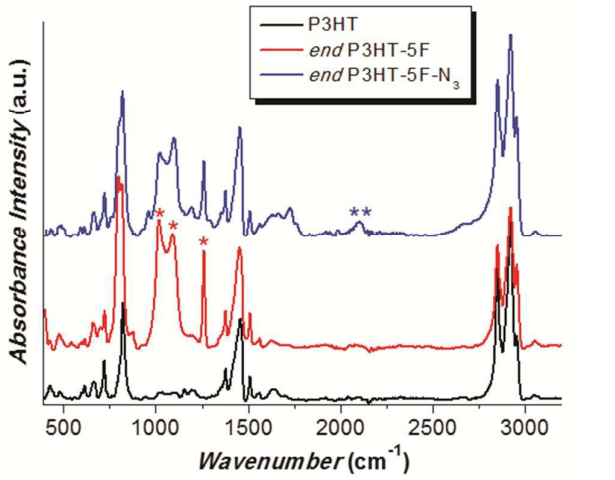

Figure 1. ATR spectra of *rr*-P3HT (black line), *end rr*-P3HT-5F (red line) with the asterisks indicating the new bands related to the perfluorophenyl ring insertion and *end rr*-P3HT-5F-N$_3$ (blue line) with the asterisks indicating the azide functionality

Table 1. SEC characterization of the *end* perfluorophenyl functionalized P3HTs at 440 nm, using CHCl$_3$ as eluent and calibration versus polystyrene standards, at room temperature

Sample	M$_n$ @440nm	PDI[l]	Respective Hybrids
P3HT-5F *Low MW*, n[a]= 6	6700	1.3	*low MW* P3HT-5F-N-C$_{70}$
P3HT-5F *Medium MW*, n[a]=12	9830	1.2	*medium MW* P3HT-5F-N-C$_{70}$ *medium MW* P3HT-5F-N-IC$_{70}$MA
P3HT-5F *High MW*, n[a]=80	12200	1.3	*high MW* P3HT-5F-N-C$_{70}$ *high MW* P3HT-5F-N-IC$_{70}$MA

[a] n values as calculated via ^{1}H NMR end group analysis.

Since polymer MW characterization via SEC inherently deviate from the true polymer characteristics due to differences in the hydrodynamic volume of the materials versus that of the polystyrene calibrants, we carried out all further calculations using the number average repeating units calculated via NMR.

Thereafter, the end-perfluorophenyl *rr*-(P3HT)$_n$-5F polymers were quantitatively transformed into azides via a nucleophilic substitution of the para fluorine atom, using sodium azide in the presence of 18-crown-6 in a THF/DMF solvent mixture,[47] resulting in the end (P3HT)$_n$-5F-N$_3$ of different MWs (n=6, n=12 and n=80) (Scheme 1). The successful azidation of the end P3HT-5Fs was confirmed using ATR and ^{15}N NMR spectroscopies (Figure 1, S9). The *low MW* fraction showed a clear peak at 2100 cm^{-1} in the ATR spectrum owing to the azide functionality[48] (Figure 1). The characteristic peak of the azide group at the ATR spectra of *medium* and *high MW* end P3HT-5F-N$_3$ was indistinguishable due to the low concentration of the azide functionality in the final polymers. However, ^{15}N NMR spectroscopy of all molecular weights of (P3HT)$_n$-5F-N$_3$ clearly showed two peaks attributed to the two different nitrogen environments of the azide functionality and thus the successful azidation in each case (Figure S9).

b) Preparation of the C$_{70}$-containing hybrids

The three different MW perfluorophenyl azide polythiophenes ((P3HT)$_n$-5F-N$_3$) were utilized in a [3+2] cycloaddition reaction with either C$_{70}$ or IC$_{70}$MA according to the method described above, providing the desired hybrid semiconducting polymers (Scheme 2, Table 1). After completion of the reaction, the resulting hybrid materials were washed thoroughly with either tetrahydrofuran (THF) in the case of C$_{70}$, or Et$_2$O in the case of IC$_{70}$MA hybrids to remove any traces of unreacted fullerenes and azide precursors.

A thorough ATR investigation of the purified hybrid materials versus the crude reaction mixtures and the initial polymer and fullerene precursors was carried out in order to assess the efficiency of the purification procedure (Figures 2 and S4-S5). The spectra of the crude (P3HT)$_n$-5F-N-C$_{70}$ hybrids (Figure 2a, black curve) show high contents of fullerenes due to the intense peaks in the area of 450-790 cm^{-1} and 1424 cm^{-1}. In the purified hybrid polymers a drastic decrease of the intensity of these peaks is observed, providing strong evidence of the successful removal of any unreacted C$_{70}$ (Figure 2a, green curve). The purification of (P3HT)$_n$-5F-N-IC$_{70}$MA hybrids was carried out in a similar manner (Figure 2b), but was less

View Article Online
DOI: 10.1039/C6RA22857G

straightforward. Due to the similar solubilities of the hybrid material and $IC_{70}MA$ in most solvents, selective removal of the unreacted $IC_{70}MA$ is trickier, particularly for lower MW fractions. Therefore additional chromatographic purification of the *medium MW* $(P3HT)_n$-5F-N-$IC_{70}MA$ (n=12) was employed to achieve complete removal of the unreacted $IC_{70}MA$ (see SI file for details).

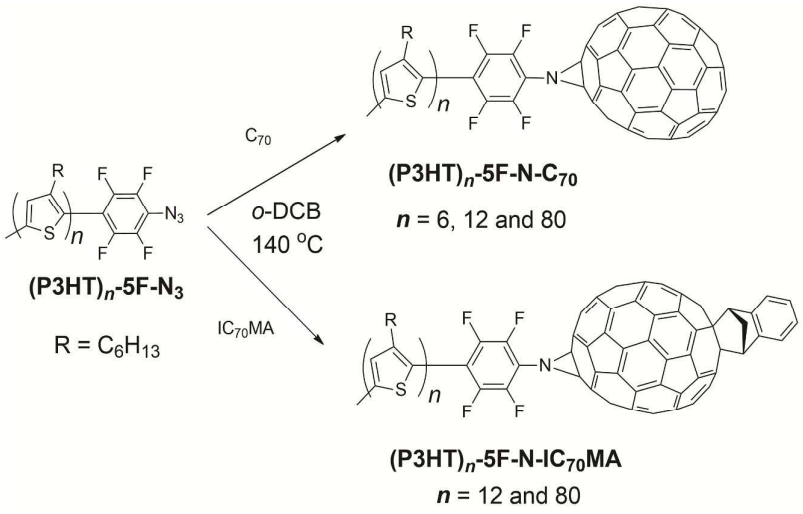

Scheme 2. [3+2] cycloaddition reaction between the P3HT-5F-N_3 and C_{70} or $IC_{70}MA$ resulting the $(P3HT)_n$-5F-N-C_{70} and $(P3HT)_n$-5F-N-$IC_{70}MA$ hybrids, respectively

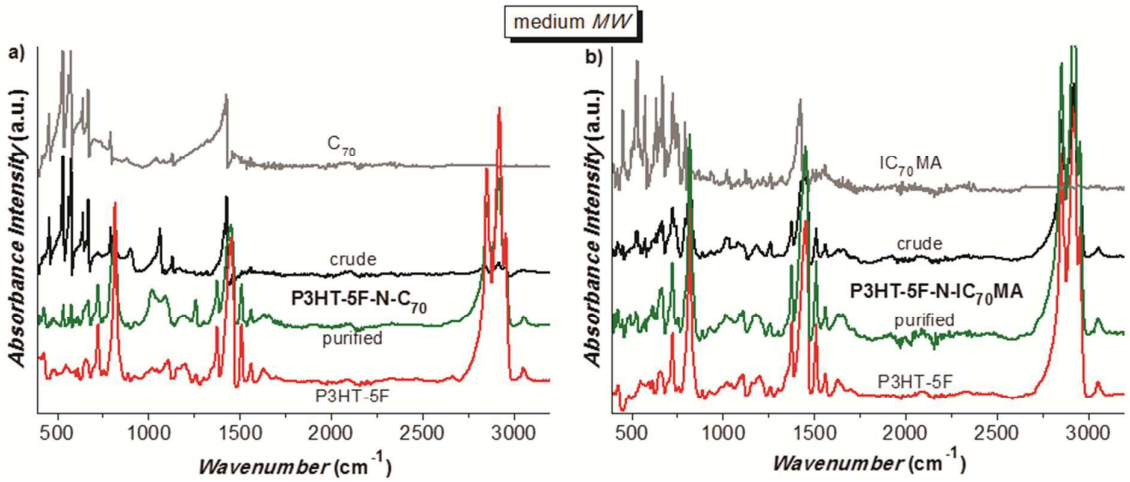

Figure 2. ATR spectra of the crude and purified *medium MW end* P3HT-5F-N-fullerene hybrids with (a) C_{70} and (b) $IC_{70}MA$ in comparison with the initial P3HT-5F and the corresponding fullerene precursors.

The resulting hybrids were characterized by MALDI TOF mass spectrometry, ^1H and ^{13}C NMR, and ATR spectroscopies. MALDI TOF mass spectra of low, medium and high MW fractions of $(P3HT)_n$-5F-N-C_{70} exhibit a very strong peak with m/z 840 corresponding to the C_{70} fragment, whereas all $(P3HT)_n$-5F-N-$IC_{70}MA$ hybrids exhibit a very strong peak with m/z 956 corresponding to the $IC_{70}MA$ unit, both unambiguously confirming the formation of the desired hybrid structures (see SI for details). The corresponding molecular ion peaks were not observed in any of the hybrids suggesting that the strain energy in the three-membered aziridine ring is high and fragmentation is more favourable than the ionization of the entire hybrid molecule, even with low laser powers.[49]

^1H NMR spectroscopy of $(P3HT)_n$-5F-N-C_{70} shows only the signals corresponding to the P3HT fragments, (Figure S10). On the other hand, the ^1H NMR spectra of the $(P3HT)_n$-5F-N-$IC_{70}MA$ hybrids additionally show a number of weak signals in the regions 3.0-5.0 ppm and 7.0-7.6 ppm characteristic of the aliphatic bridge protons and of the aromatic protons of the indene functional group on the $IC_{70}MA$ fragment, respectively. These signals are not present in neither the end-P3HT-5F precursors, nor in the C_{70}-containing hybrids $(P3HT)_n$-5F-N-C_{70}, additionally confirming the successful introduction of the $IC_{70}MA$ functionality (Figures S11-S12). Furthermore, ^{13}C NMR spectroscopy characterization of both *low MW* P3HT-5F-N-C_{70} and *medium MW* P3HT-5F-N-$IC_{70}MA$ presents conclusive

View Article Online
DOI: 10.1039/C6RA22857G

evidence of the successful functionalisation of the polymer chain with the fullerene cage (Figure 3). Both the C_{70} and $IC_{70}MA$ containing hybrids show the characteristic signals of the *rr*-P3HT backbone in 139.94, 133.75, 130.55, 128.67 ppm region. The ^{13}C NMR spectrum of the *low MW* P3HT-5F-N-C_{70} shows ~30 additional peaks of lower intensity, compared to the initial P3HT in the 120-150 ppm region confirming the successful functionalisation of the C_{70} cage as well as the formation of the hybrid structure. The ^{13}C NMR spectrum of the medium MW P3HT-5F-N-$IC_{70}MA$ hybrid exhibits a higher number of fullerene related signals (over 30 peaks in the region 120-150 ppm). This is consistent with the lower symmetry of the bis-functionalized C_{70} cage and potential presence of more than one regioisomers and this unambiguously confirms the proposed structure. Unfortunately, for the higher MW polymeric hybrids the fullerene signals could not be clearly distinguished due to the low relative fraction of the fullerenes in those samples.

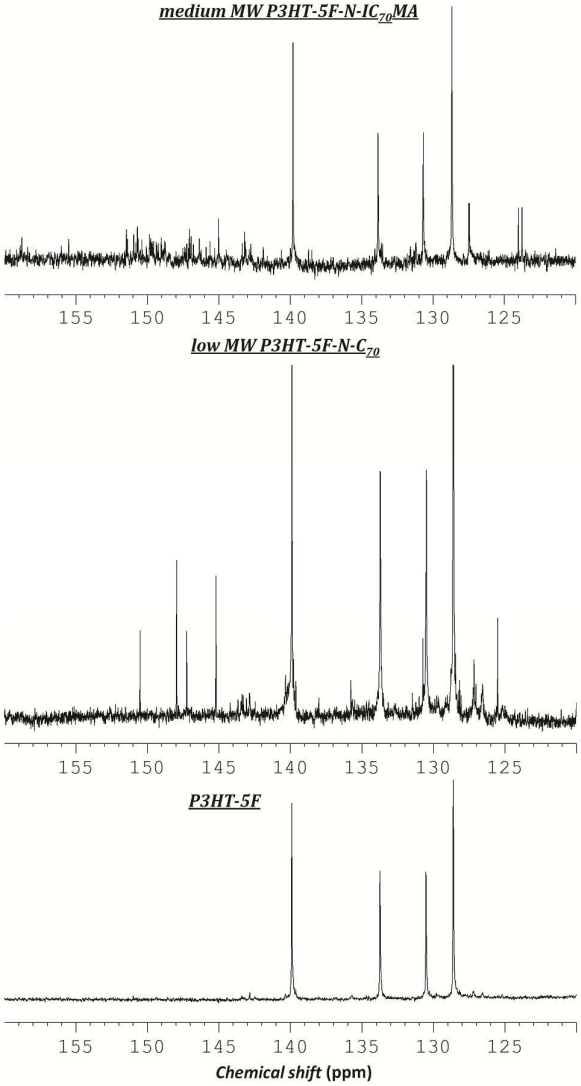

Figure 3. ^{13}C NMR spectra of the $(P3HT)_n$-5F the *low MW* $(P3HT\text{-}5F)_n$-N-C_{70} hybrid and the *medium MW* $(P3HT)_n$-5F-N-$IC_{70}MA$ hybrid, recorded in $CDCl_3$.

3.2 Electronic properties of the P3HT-5F-N-C_{70} and P3HT-5F-N-$IC_{70}MA$ hybrids.

The UV-Vis and PL spectra of all *end* $(P3HT)_n$-5F-C_{70} and *end* $(P3HT)_n$-5F-N-$IC_{70}MA$ hybrids were recorded in toluene solutions as well as in film form. The UV-Vis spectra of all hybrid materials in solutions essentially comprise a superposition of the characteristic absorption peaks of the P3HT and the fullerene components (Figure 4). The strong P3HT absorption dominates the spectrum in each case, with the absorbance maximum slightly red shifted with the increase of the molecular weight: 440 nm in the *low MW*, 450 nm in the *medium MW* and at 460 nm in the *high MW* polymer, respectively. Additionally, both C_{70}- and $IC_{70}MA$- tagged hybrids exhibit the characteristic absorbance bands of the C_{70} cage, showing transitions at 335, 363, 382 and 600 nm in the former and at 350, 400 and 560 nm in the latter structures. These absorption bands are notable in both *low* and *medium MW* fractions, and are undistinguishable in the *high MW* fraction due to the low ratio of the fullerene unit over the polymer within these hybrids (Figure 4a and 4b).

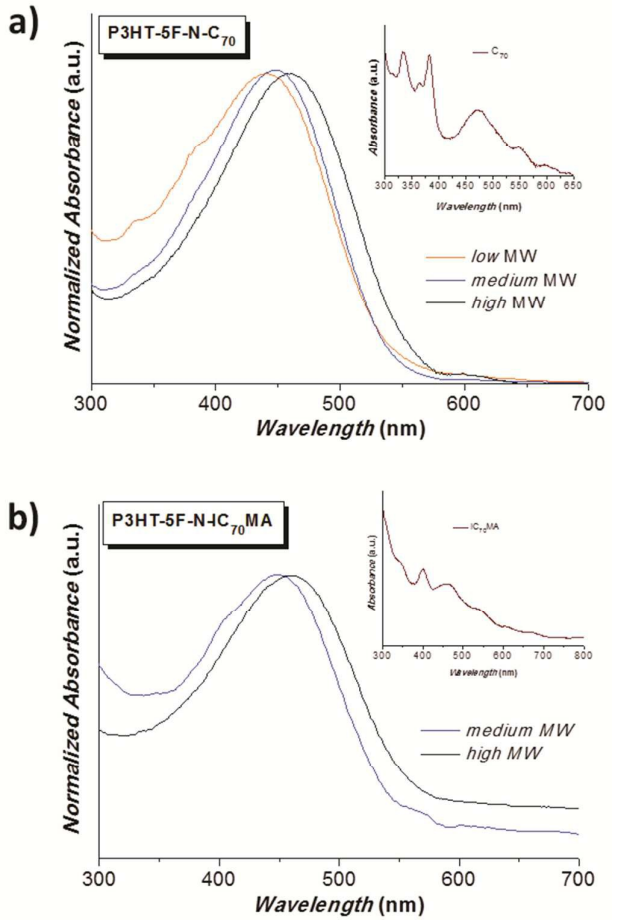

Figure 4. Normalized absorption spectra of different molecular weight a) *end* $(P3HT)_n$-5F-C_{70} hybrids and b) *end* $(P3HT)_n$-5F-$IC_{70}MA$ hybrids, recorded in toluene solutions (insets show absorption spectra of fullerene C_{70} and $IC_{70}MA$ in toluene respectively).

View Article Online
DOI: 10.1039/C6RA22857G

The photoluminescence (PL) spectra of all *end* $(P3HT)_n$-5F-hybrids in toluene solutions (Figures S13-S15) after excitation at 440 nm corresponding to the P3HT absorption maximum, showed the characteristic photoluminescence peaks of the poly(thiophene) segments, however no quenching of the luminescence in the hybrid polymeric materials. The absorption (Figure 5, 6a) and emission spectra (Figures 6b, S16-S17) of all *end* $(P3HT)_n$-5F-hybrid materials have also been recorded in film form. Similarly to the solution spectra, the absorption spectrum of each polymeric material shows the strong characteristic absorbance of the P3HT backbone, as well as weaker characteristic absorbance peaks of the functionalized C_{70} in the 200-400 nm region (Figure 5).

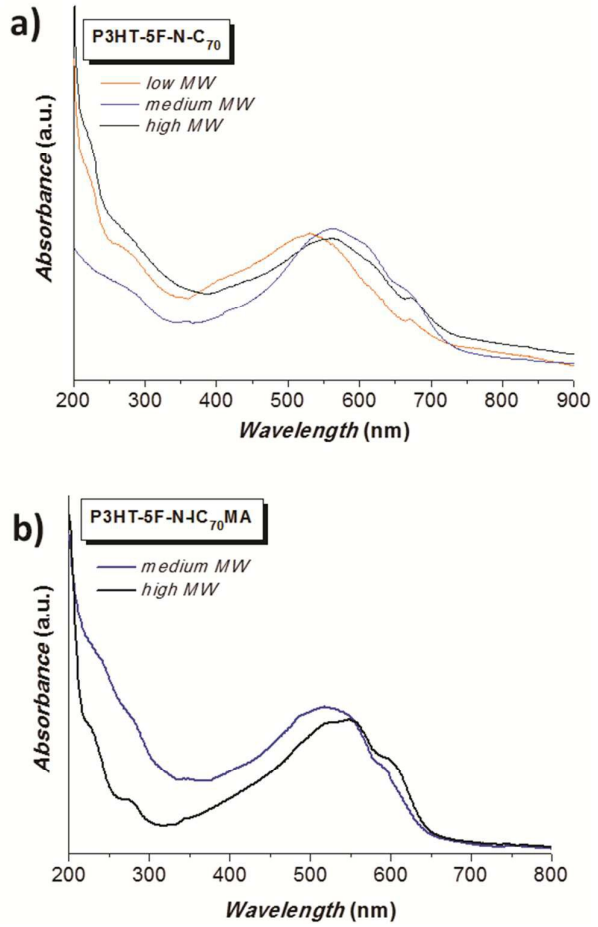

Figure 5. Absorption spectra of the a) all *end* $(P3HT)_n$-5F-N-C_{70} hybrids, b) all *end* $(P3HT)_n$-5F-N-$IC_{70}MA$ hybrids, recorded in film form.

In contrast, the photoluminescence spectra of $(P3HT)_n$-5F-N-C_{70} and $(P3HT)_n$-5F-N-$IC_{70}MA$ recorded in film form, upon excitation at 520 nm, showed small but notable differences compared to the solution measurements (Figures 6b, S16-S17). The *medium* and *high MW* $(P3HT)_n$-5F-N-$IC_{70}MA$ (Figures S17b, 6b) as well as the *high MW* $(P3HT)_n$-5F-N-C_{70} hybrid films (Figure 6b) showed notable decrease of the photoluminescence intensity. Whereas the PL intensity in the *low* and *medium* MW $(P3HT)_n$-5F-N-C_{70} slightly increased compared to their analogous fullerene-free precursors (Figures S16b-S17b). Such non-linear behaviour may be related to the changes in the film structure of the different hybrid materials, as well as the known concentration dependence of the P3HT photoluminescence intensity.[50]

However, some degree of electronic interactions between the $IC_{70}MA$ component and the P3HT backbone cannot be excluded, as well as possible non-uniformity in the film thickness between the different samples. In all hybrid polymer cases, however, a total PL quenching is not anticipated since the weight fraction of the fullerene species is below that of the P3HT weight fraction. The P3HT absorption maxima are slightly red shifted with the increasing molecular weight of the sample, following the same trend as observed in solution.

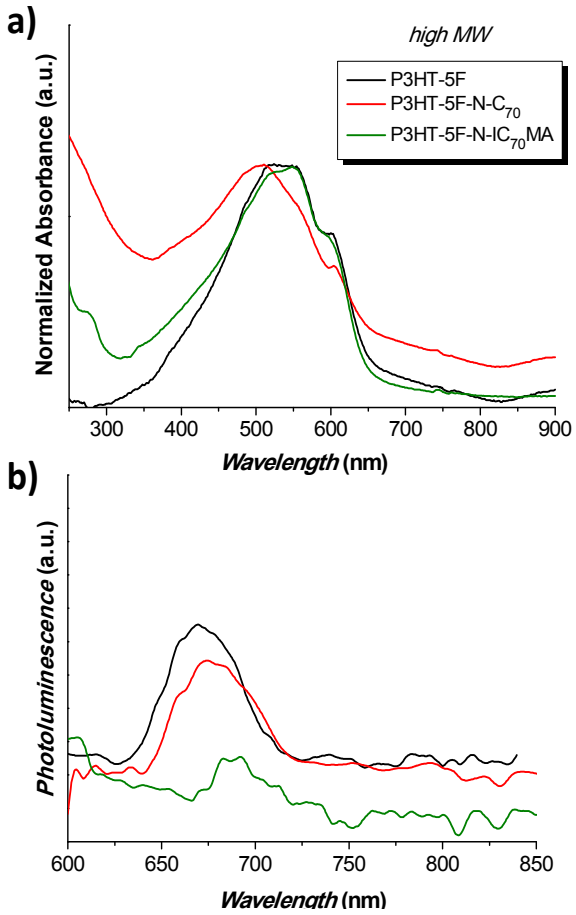

Figure 6. (a) Normalized absorption spectra and (b) Photoluminescence spectra, upon excitation at 520 nm, of the *high MW end* $(P3HT)_n$-5F-N-C_{70} and $(P3HT)_n$-5F-N-$IC_{70}MA$ hybrids, recorded in film form.

C_{70} fullerene exhibits a characteristic emission in the 700-750 nm region, the peak position of which depends on the functionalisation pattern of the fullerene cage and can shift slightly upon functionalisation providing thus, useful structural information. However, the quantum yield of this emission is extremely low and normally has values of $x10^{-4}$.[51,52] On the contrary, P3HT is a strong fluorophore, with a broad emission peak centred around 550 nm and a quantum yield of 10^{-2},[53]

View Article Online
DOI: 10.1039/C6RA22857G

which is two orders of magnitude higher than the fullerene emission. Figure S18 shows photoluminescence maps of $IC_{70}MA$ (a), $(P3HT)_n$-5F (n=6) (b), and $(P3HT)_n$-5F-N-$IC_{70}MA$ (n=12) (c) recorded in toluene solutions of similar concentrations and centred around the 650-750 nm emission region where the fullerene photoluminescence is expected. Although the maximum of P3HT photoluminescence is well outside of this region, the tail of its emission peak is still visible (Figure S18b) and has relatively strong intensity compared to the $IC_{70}MA$ (Figure S18a). As a result, the photoluminescence map of the hybrid material (Figure S18c) is dominated by the emission of the P3HT backbone, and the fullerene-related emission cannot be distinguished, therefore making any further structural conclusions unfeasible.

Table 2. Electrochemical data[a] for the *end* $(P3HT)_n$-5F-C_{70} and $(P3HT)_n$-5F-$IC_{70}MA$ hybrids and the corresponding *end* $(P3HT)_n$-5F fullerene-free precursors

Sample		$E_{1/2}^{red1}$	$E_{1/2}^{red2}$	$E_{1/2}^{red3}$	E_{onset}^{ox}
end $(P3HT)_n$-5F	*low MW n=6*	-	-	-	0.17
	high MW n=80	-	-	-	0.11
$(P3HT)_n$-5F-N-C_{70}	*low MW n=6*	-1.01 (0.07)	-1.41 (0.08)	-1.83 (0.08)	0.17
	medium MW n=12	-1.01 (0.07)	-1.39 (0.07)	-1.80 (0.06)	0.09
	high MW n=80	-1.02 (0.07)	-1.40 (0.07)	-1.80 (0.07)	0.08
$(P3HT)_n$-5F-N-$IC_{70}MA$	*medium MW n=12*	-1.14 (0.09)	-1.51 (0.09)	-1.89 (0.09)	0.09
	high MW n=80	-1.14 (0.07)	-1.51 (0.07)	-1.87 (0.08)	0.08

[a] Potentials ($E_{1/2}$ = (Epa + Epc)/2) in V quoted to the nearest 0.01 V. All potentials are reported against the Fc^+/Fc couple for 0.5 – 1.0 mM solutions in o-DCB containing 0.2 M [^{n}Bu$_4$N][BF_4] as the supporting electrolyte. The anodic/cathodic peak separation (ΔE = Epa – Epc) is given in brackets where applicable.

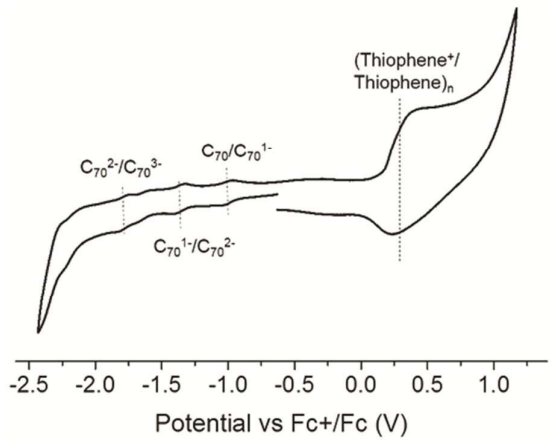

Figure 7. Cyclic voltammogramm of *low MW* P3HT-5F-N-C_{70} recorded in *o*-DCB containing 0.2 M [^{n}Bu$_4$N][BF_4] as supporting electrolyte at 0.1 V/s.

To get a further insight into the electronic properties of the resulting hybrids cyclic voltammetric analysis has also been performed. The cyclic voltammogramms have been recorded in *o*-DCB solutions containing 0.2 M [nBu_4N][BF_4] as supporting electrolyte at 0.1 V/s. The observed redox potentials for each hybrid are summarized in Table 2 and an example of a typical CV is given in Figure 7, while the voltamograms of the remaining materials are presented in Figures S19-S21. Each of the hybrid polymers as well as their perfluorinated precursors exhibit a set of several broad overlapping irreversible oxidation processes in the range from +0.08 to +0.70 V corresponding to the sequential oxidation of a number of P3HT units.[54] The intensity and the position of the onset potential of this process vary from the low to medium and high MW fractions.[55,56,57] Moreover, each of the fullerene-containing hybrids (P3HT)n-5F-N-C_{70} and $(P3HT)_n$-5F-N-$IC_{70}MA$ also shows three quasi-reversible reduction processes, significantly lower in intensity than the P3HT oxidation (Figure 7 and S20-S21). These reduction processes are observed at -1.01/-1.02, -1.39/-1.41 and -1.80/-1.83 V in all (P3HT)n-5F-N-C_{70}, and at -1.14, -1.51 and -1.87/-1.89 V in all (P3HT)n-5F-N-$IC_{70}MA$ hybrids. Comparison of the redox potentials of the corresponding hybrids (Table 2) with the unfunctionalised C_{70}, indene-C_{70} monoadduct ($IC_{70}MA$) and a C_{70}-indene bis-adduct ($IC_{70}BA$)[20] suggests that these one-electron reduction processes most likely correspond to the sequential fullerene cage reductions C_{70}/C_{70}^{1-}, C_{70}^{1-}/C_{70}^{2-} and C_{70}^{2-}/C_{70}^{3-}, respectively.

Each of the reduction processes is slightly shifted towards more negative values in $(P3HT)_n$-5F-N-$IC_{70}MA$ as compared to $(P3HT)_n$-5F-N-C_{70} hybrids which is characteristic of the increasing degree of functionalization of the fullerene cage.[20] Notably, the fullerene-related processes are observed in all hybrid samples regardless of the molecular weight, although their intensity decreases as the molecular weight increases (Figure S20).

3.3. Morphology of the P3HT-fullerene hybrids.

Thin film morphology of all end P3HT-5F and their respective fullerene-containing hybrids was probed by transmission electron spectroscopy (TEM) (Figures 8, S22). The functionalised end $(P3HT)_n$-5F polymers exhibit formation of homogeneous thin films whereas their corresponding fullerene-containing hybrids ($(P3HT)_n$-5F-N-C_{70} and $(P3HT)_n$-5F-N-$IC_{70}MA$) show higher nanophase separation due to the fullerene's attachment. Notably, neither of the hybrids displayed any aggregates formation.

As the molecular weight of the end $(P3HT)_n$-5F increases, the films present better organization and thus formation of larger domains. The *low MW* P3HT-5F-N-C_{70} hybrid showed a more phase separated thin film compared to its fullerene-free polymer with notable crystallization of the P3HT chains as evident from the grey rod like structures (Figure S22). On the contrary, the *medium* and *high MW* $(P3HT)_n$-5F-N-C_{70} hybrids showed formation of uniform films with extended phase separation compared to their corresponding end $(P3HT)_n$-5F polymeric precursors, with the domain size increasing from the medium to high MW fraction. The films of both *medium* and

View Article Online
DOI: 10.1039/C6RA22857G

high MW $IC_{70}MA$-containing hybrids $(P3HT)_n$-5F-N-$IC_{70}MA$ also showed notable change in the morphology compared to their initial fullerene-free analogues resulting in higher nanophase separated thin films. However, the domain size of the $IC_{70}MA$-tagged hybrids is smaller than of their respective end $(P3HT)_n$-5F-C_{70} hybrids. This is related to the effect of indene functional group which is known to improve the miscibility of the fullerene with the P3HT polymer[58] therefore resulting in improved, nanostructured and homogeneous film formation.

More particularly, quantitative statistical analyses of the hybrids' TEM images revealed that the dark regions, identified as C_{70}-rich regions, in the *medium* and *high MW* $(P3HT)_n$-5F-N-C_{70} hybrids are of 0.7-2 nm and 1.4-3.5 nm size, respectively. For the $IC_{70}MA$ *medium* and *high MW* hybrids, the dark fullerene rich regions are of 0.5-2 nm size in both cases.

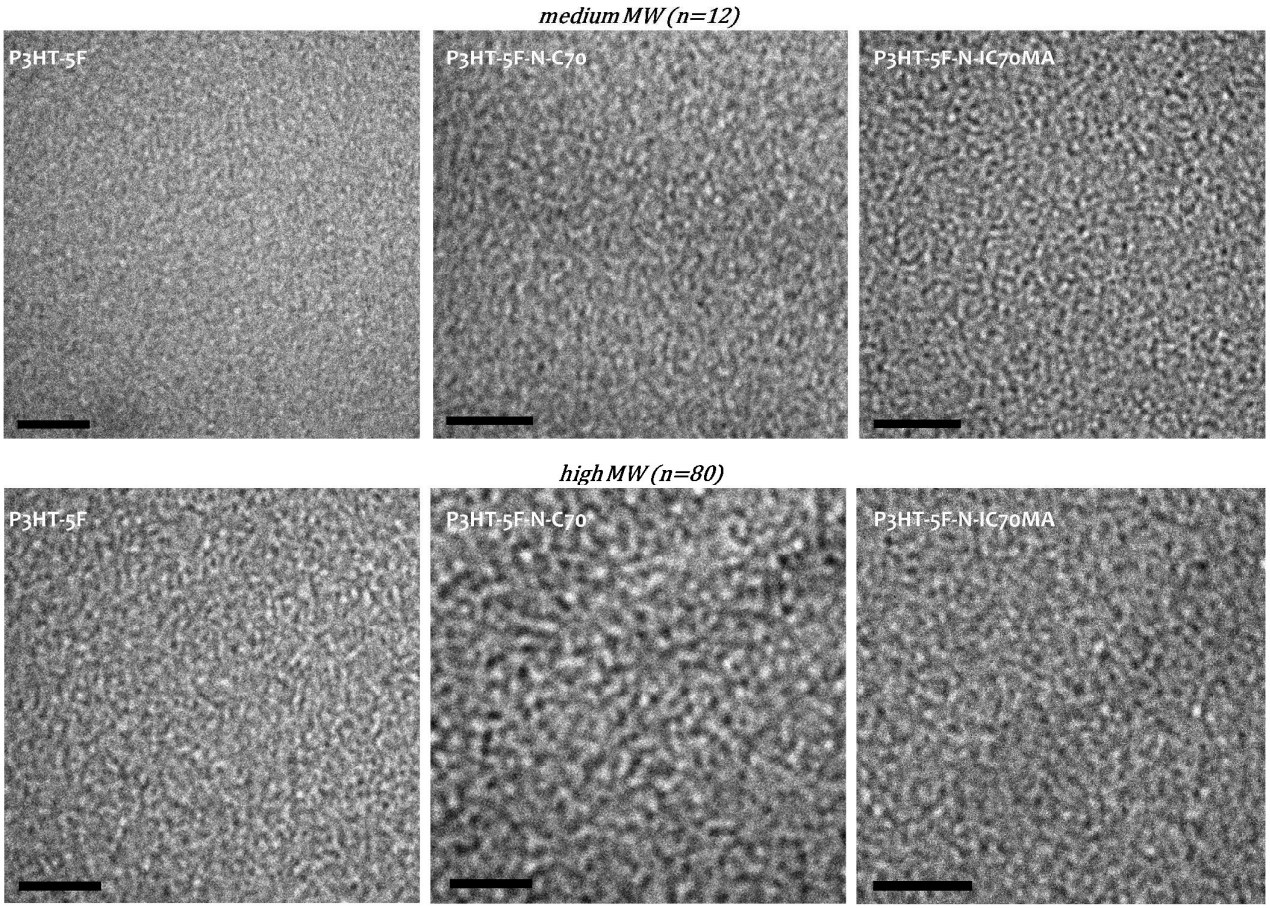

Figure 8. TEM images of *medium and high MW end*-$(P3HT)_n$-5F, $(P3HT)_n$-5F-N-C_{70} and $(P3HT)_n$-5F-N-$IC_{70}MA$ hybrids obtained by drop casting dilute solution of the corresponding polymer in *o*-DCB on the TEM grid without any thermal treatment (scale bar 20 nm).

Conclusions

An efficient route to synthesize hybrid additives for the P3HT:$IC_{70}BA$ based BHJ OPV devices has been developed. The three-step synthetic procedure is based on the in situ introduction of a pentafluorophenyl moiety to the ω end position of the polythiophene backbone during the polymerisation step, followed by the substitution of the para fluorine atom with a functional azide group. The azide-functionalized P3HT polymers are then reacted with pristine C_{70} or indene-C_{70} monoadduct ($IC_{70}MA$) via a [3+2] cycloaddition reaction providing the corresponding hybrid materials. The synthetic procedure has been tailored to tune the molecular weight of the resulting polymer, yielding structures with the polythiophene chain varying from 6 to 80 thiophene repeating units and the subsequent introduction of both unfunctionalised C_{70} and indene-C_{70} monoadduct ($IC_{70}MA$).

The properties of the resulting hybrid structures have been thoroughly investigated showing that the electronic properties of the P3HT polymer are largely unaffected by the introduction of the fullerene cage at the end position of the polymeric chain. The morphology of the resulting hybrid materials is notably different from the fullerene-free analogues, showing an enhanced nanophase separation. The domain sizes in all C_{70}-containing hybrids are notably larger than in the $IC_{70}MA$-

View Article Online
DOI: 10.1039/C6RA22857G

containing hybrids, demonstrating the importance of the indene functional group in tuning the morphology of the resulting films. Due to their unique electronic and morphological properties the hybrid polymers reported in this study are expected to improve and stabilize the morphology of the P3HT:$IC_{70}BA$ photoactive blend, which becomes more and more widely used to produce highly efficient and cheap large scale OPV devices. The addition of small quantities of these hybrids as compatibilising additives into the P3HT:$IC_{70}BA$ blend may allow better control over the film morphology of the active layer whilst not perturbing the electronic structure of the blend.

Acknowledgements

The authors thank Dr. D. Vachliotis of the Instrumental Analysis Laboratory, University of Patras for his efforts during the NMR experiments and Dr Maria Kollia from the Laboratory of Electron Microscopy and Microanalysis at the University of Patras for the TEM images
The present work was funded from the European Union's Seventh Framework Programme (FP7/2007-2013) under the grant agreement No 310229 - FP7-NMP-Large-2012.1.4-1 and the acronym "Smartonics - Development of smart machines, tools and processes for the precision synthesis of nanomaterials with tailored properties for Organic Electronics".

References

1 K. A. Mazzio and C. K. Luscombe, *Chem. Soc. Rev.*, 2015, **44**, 78-90.
2 S. H. Park, A. Roy, S. Beaupré, S. Cho, N. Coates, J. S. Moon, D. Moses, M. Leclerc, K. Lee and A. J. Heeger *Nat. Photonics*, 2009, **5**, 296-302.
3 C. Sekine, Y. Tsubata, T. Yamada, M. Kitano and S. Doi, *Sci, Technol. Adv. Mater*., 2014, **15**, 034203-034218.
4 C .J. Brabec, S. Gowrisanker, J.J.M. Halls, D. Laird, S. Jia and S. P. Williams, *Adv. Mater*., 2010, **22**, 3839-3856.
5 L. Lu, T. Zheng, Q. Wu, A. M. Schneider, D. Zhao and L. Yu, *Chem. Rev*., 2015, **115**, 12666−12731.
6 M. Brinkmann, *J. Polym. Sci. Part B Polym. Phys.*, 2011, **49**, 1218–1233.
7 J. Chen and Y. Cao, *Acc. Chem. Res.*, 2009, **42**, 1709-1718.
8 R. Kroon, M. Lenes, J. C. Hummelen , P. W. M. Blom and B. de Boer, *Polymer Reviews*, 2008, **48**, 531–582.
9 U. Mehmood, A. Al-Ahmed and I. A.Hussein, *Renew. Sustainable Energy Rev*., 2016, **57**, 550–561.
10 Y. He and Y. Li, *Phys. Chem. Chem. Phys*., 2011, **13**, 1970–1983.
11 W. Ma , C. Yang, X. Gong, K. Lee and A. J. Heeger, *Adv. Funct. Mater*., 2005, **15**, 1617-1622.
12 B. Kadem, A. Hassan and W. Cranton, *J Mater Sci: Mater Electron*, DOI 10.1007/s10854-016-4661-8.
13 Y. Zhao, Z. Xie, Y. Qu, Y. Geng and L. Wang, *Appl. Phys. Lett.*, 2007, **90**, 043504.
14 A. J. Moulé and K. Meerholz, *Adv. Mater.*, 2008, **20**, 240-245.
15 Y. Yao, J. Hou, Z. Xu, G. Li and Y. Yang, *Adv. Funct. Mater.,* 2008, **18**, 1783-1789.
16 Y. Li, *Chem. Asian J*., 2013, **8**, 2316-2328.
17 N.C. Miller, S. Sweetnam, E.T. Hoke, R. Gysel, C. E. Miller, J. A. Bartelt, X. Xie, M. F. Toney and M. D. McGehee, *Nano Lett.,* 2012, **12**, 1566-1570.
18 H. Kang, C.-H. Cho, H.-H. Cho, T. E. Kang, H. J. Kim, K.-H. Kim, S. C. Yoon and B. J. Kim, *ACS Appl. Mater. Interfaces,* 2012, **4**, 110-116.
19 Y. He, H.-Y. Chen, J. Hou and Y. Li, *J. Am. Chem. Soc*., 2010, **132**, 1377-1382.
20 Y. He, G. Zhao, B. Peng and Y. Li, *Adv. Funct. Mater.,* 2010, **20**, 3383-3389.
21 Y. Sun, C. Cui, H. Wang and Y. Li, *Adv. Energy Mater*., 2011, **1**, 1058-1061.
22 X. Guo, C. Cui, M. Zhang, L. Huo, Y. Huang, J. Hou and Y. Li, *Energy Environ. Sci*,. 2012, **5**, 7943-7949.
23 X. Fan, C. Cui, G. Fang, J. Wang, S. Li, F. Cheng, H. Long and Y. Li, *Adv. Funct. Mater*., 2012, **22**, 585-590.
24 X. Zhou, X. Fan, X. Sun, Y. Zhang and Z. Zhu, *Nanoscale Res. Lett.,* 2015, **10**:29.
25 J. K. Kallitsis, C. Anastasopoulos and A. K. Andreopoulou, *MRS Communications*, 2015, **5**, 365–382.
26 G. Wantz, L. Derue, O. Dautel, A. Rivaton, P. Hudhomme and C. Dagron-Lartigau, *Polym Int.,* 2014, **63***,* 1346-1361.
27 J. S. Kim, Y. Lee, J. H. Lee, J. H. Park, J. K. Kim and K. Cho, *Adv. Mater*., 2010, **22**, 1355-1360.
28 M. Jeffries-El, G. Sauvé and R. D. McCullough, *Adv. Mater*., 2004, **16**, 1017-1019.
29 Y. Chen, C. Zhan and J. Yao, *Chem. Asian J.* 2016, doi: 10.1002/asia.201600374
30 S. Th. Salammal, J. Chen, F. Ullah and H, Chen, *J Inorg Organomet. Polym.*, 2015**, 25***,* 12–26.
31 K. Yuan, L. Chen and Y. Chen, *Polym Int.,* 2014, **63***,* 593–606.
32 J. U. Lee, J. W. Jung, T. Emrick, T. P. Russell and W. H. Jo, *J. Mater. Chem.,* 2010, **20**, 3287-3294.
33 J. U. Lee, J. W. Jung, T. Emrick, T. P. Russell and W. H. Jo, *Nanotechnology,* 2010, **21**, 105201-105210.
34 A. A. Stefopoulos, C. L. Chochos, M. Prato, G. Pistolis, K. Papagelis, F. Petraki, S. Kennou and J. K. Kallitsis, *Chem. Eur. J.*, 2008, **14**, 8715–8724.
35 D. A. Kamkar, M. Wang, F. Wudl and T.-Q. Nguyen, *ACS Nano*, 2012, **6**, 1149-1157.
36 V. Gernigon, P. Lévêque, F. Richard, N. Leclerc, C. Brochon, C. H. Braun, S. Ludwigs, D. V. Anokhin, D. A. Ivanov, G. Hadziioannou and T. Heiser, *Macromolecules,* 2013, **46**, 8824−8831.
37 A. Laiho, R.H. A. Ras, S. Valkama, J. Ruokolainen, R. Österbacka and O. Ikkala, *Macromolecules*, 2006, **39**, 7648-7653.

View Article Online
DOI: 10.1039/C6RA22857G

38 S.-L. Hsu, C.-M. Chen, Y.-H. Cheng and K.-H Wei, *J. Polym. Sci. Part A Polym. Chem,* 2011, **49**, 603–611.
39 L. Perrin, M. Legros and R Mercier, *Macromolecules*, 2015, **48**, 323–336.
40 B Yameen, T Puerckhauer, J Ludwig, I Ahmed, O Altintas, L Fruk, A. Colsmann and C. Barner-Kowollik, *Small,* 2014, **10**, 3091–3098.
41 S. Kakogianni, S. N. Kourkouli, A. K. Andreopoulou and J. K. Kallitsis, *J. Mater. Chem. A*, 2014, **2**, 8110–8117.
42 L. Sygellou, S. Kakogianni, A. K. Andreopoulou, K. Theodosiou, G. Leftheriotis, J. K. Kallitsis and A. Siokou, *Phys. Chem. Chem. Phys.*, 2016, **18**, 4154-4165
43 F. Richard, C. Brochon, N. Leclerc, D. Eckhardt, T. Heiser and G. Hadziioannou, *Macromol. Rapid Commun*., 2008, **29**, 885–891.
44 C. A. Schneider, W. S. Rasband and K. W. Eliceiri, *Nature Methods,* 2012, **9**, 671-675.
45 M. D. Abramoff, P. J. Magalhaes and S. J. Ram, *Biophotonics International*, 2004, **11**, 36-42.
46 P. Giannopoulos, A. Nikolakopoulou, A. K. Andreopoulou, L. Sygellou, J. K. Kallitsis and P. Lianos, *J. Mater. Chem. A*, 2014, **2**, 20748-20759.
47 H. J. Kim, A-R. Han, C.-H. Cho, H. Kang, H.-H. Cho, M. Y. Lee, J. M. J. Frechet, J. H. Oh and B. J. Kim, *Chem. Mater*., 2012, **24**, 215–221.
48 L.-H. Liu and M. Yan, *Acc. Chem. Res.,* 2010, **43**, 1434–1443.
49 J. B. Sweeney, *Chem. Soc. Rev.*, 2002, **31**, 247–258.
50 P.-T. Huang, P.-F. Huang, Y.-J. Horng and C.-P. Yang, *J. Chin. Chem. Soc*., 2013, **60**, 467-472.
51 J. W. Arbogast and C. S. Foote, *J. Am. Chem. Soc.*, 1991, **113**, 8886-8889.
52 B. Ma and Y.-P. Sun, *J. Chem. Soc., Perkin Trans.*, 1996, **2**, 2157-2162.
53 B. Xu and S. Holdcroft, *Macromolecules,* 1993, **26**, 4457-4460.
54 J. Hou, Z. Tan, Y. Yan, Y. He, C. Yang and Y. Li, *J. Am. Chem. Soc.,* 2006, **128**, 4911-4916.
55 K. Tremel and S. Ludwigs, *Adv. Polym. Sci*., 2014, **265**, 39–82.
56 M. Trznadel, A. Pron, M. Zagorska, R.Chrzaszcz and J. Pielichowski, *Macromolecules* 1998, **31**, 5051-5058.
57 M. Skompska and A. Szkurłat, *Electrochimica Acta*, 2001, **46**, 4007–4015.
58 A. A. Y. Guilbert, L. X. Reynolds, A. Bruno, A. MacLachlan, S. P. King, M. A. Faist, E. Pires, J. Emyr Macdonald, N. Stingelin, S. A. Haque and J. Nelson, *ACS Nano*, 2012, **6**, 3868-3875.

View Article Online
DOI: 10.1039/C6RA22857G

Table of Contents entry

Semiconducting End-Perfluorinated P3HT-Fullerenic Hybrids as Potential Additives for P3HT/$IC_{70}BA$ blends

S. Kakogianni, M. A. Lebedeva, G. Paloumbis, A. K. Andreopoulou, K. Porfyrakis, and J. K. Kallitsis

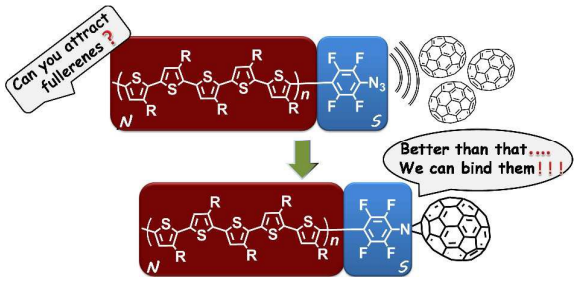

Hybrid materials based on polythiophene-fullerene species covalently attached through aziridine bridges are presented, as potential stabilizers of P3HT:$IC_{70}BA$ active layers for BHJ devices.